Kurzzusammenfassung

Seit der Entdeckung des [2.2]Paracyclophans vor exakt 70 Jahren durch Brown und Fathing[1] entfachte diese Verbindung großes Interesse in der Wissenschaft. Die zwei zueinander coplanar angeordneten Benzole mit einem sehr geringen Abstand von 3.09 Å,[2-3] die durch zwei zueinander in *para*-Position stehenden Ethylbrücken verbrückt werden, ergeben ein gespanntes und verzerrtes "*bent and battered*"[2] Grundgerüst, so wie es in der klassischen, nichtcyclophanischen Aromatenchemie unbekannt ist. Die besonderen Eigenschaften dieses Moleküls sind I) die einzigartige transannulare elektronische Kommunikation der zwei π -Systeme ermöglicht durch den besonders geringen Benzolringabstand, [4-5] II) die Präsenz einer planaren Chiralität bei Funktionalisierung und III) der beträchtliche sterische Raumanspruch durch die Ethylbrücken und den coplanar liegenden zweiten Benzolring. Aufgrund dieser besonderen Eigenschaften ist dieses Molekül synthetisch anspruchsvoll, da die verbogene und gespannte Struktur die Chemie in besonderer Weise beeinflusst. Bis zum heutigen Tage wurde das [2.2]Paracyclophangerüst hauptsächlich in der Katalyse als chiraler Ligand erforscht. Im Gegensatz dazu sind Untersuchungen zu materialwissenschaftlichen Anwendungen sehr viel seltener berichtet.[6]

Daher ist das Ziel dieser Arbeit synthetische Zugänge zu mehreren [2.2]Paracyclophan-basierten Derivaten zu finden die es mehreren Materialwissenschaftlichen Anwendungen und der Supramolekularen Chemie ermöglicht die transannulare Kommunikation, den besonderen sterischen Raumanspruch und die Chiralität auszunutzen.

Die transannulare elektronische Kommunikation wurde für das Design von neuartigen Luminophoren genutzt um sogenannte *thermally activated delayed fluorescence* (TADF) Emitter darzustellen. Es konnten aus einer Reihe von zehn dargestellten Zielstrukturen zwei blau emittierende Moleküle gewonnen werden die den TADF Mechanismus zur effizienten Lichterzeugung nutzen.

Der besondere Raumanspruch wurde genutzt um [2.2]Paracyclophan-basierte (1,4)Carbazolophan-analoga zum im Emitterdesign gängigen Carbazol darzustellen. Der dargestellte TADF Emitter besaß die erwartete erhöhte Torsion, welche TADF Emission ermöglichte. Dies erlaubte eine OLED mit einem EQE_{max} von 17% herzustellen.

Desweiteren wurde die Untersuchung des Chiralitätstransfers von einem Molekül mittels chemischer Gasphasenabscheidung generierten Poylmerfasern durch die geeigneter chiraler [2.2]Paracyclophan-basierter Monomere ermöglicht.

Schließlich konnte durch die Synthese eines geeigneten [2.2]Paracyclophanderivates die Voraussage, dass das sphärische Grundgerüst ein vielversprechender Gast in der supramolekularen Wirts-Gast Chemie ist.

Während all dieser synthetischen Problemstellungen wurden die Besonderheiten der [2.2]Paracyclophan weiter erforscht. So wurde eine neuartige *para*-selektive C–H Aktivierung und die Darstellung eines neuartigen (1,7)Carbazolophans untersucht.

Abstract

Since the first discovery of [2.2]paracyclophane by Brown and Farthing exactly 70 years ago[1] this molecule has sparked tremendous interest in the scientific community. The two coplanar phenyl rings are in close proximity of 3.09 Å,[2-3] fixed by two short ethyl bridges in *para*-position resulting in a "*bent and battered*"[2] molecular skeleton which is unknown in conventional non-cyclophane aromatic chemistry. The key features of this molecule are I) the unique electronic situation enabling transannular electronic communication of the two π -systems,[4-5] II) the presence of planar chirality upon substitution and III) the considerable spherical bulk induced by the adjacent ethyl bridge and second co-planar phenyl ring. Despite these unique features, the bent and therefore unfavored conformation influences the chemistry of this molecule dramatically, making the synthetic derivatization a challenging endeavor. Up until now the [2.2]paracyclophane scaffold has predominantly been investigated in the context of catalysis as a chiral ligand,[7-9] utilizing the chirality and steric hindrance of this molecule. In contrast, investigations regarding material sciences are far less explored.[6]

Therefore, the aim of this thesis was to establish a synthetic access to a variety of [2.2]paracyclophane-based derivatives for different applications in material sciences and supramolecular chemistry exploiting transannular communication, steric demand and chirality.

For the design of luminescent molecules, the through-space electronic communication of the [2.2]paracyclophane scaffold was taken advantage of, and the promising thermally activated delayed fluorescence (TADF) mechanism for efficient light generation was established, giving two blue emitters out of ten synthesized target structures for which the TADF relaxation principle was verified.

The exceptional steric demand was utilized to generate a [2.2]paracyclophane-based (1,4)carbazolophane analogue of the common carbazole group for TADF emitter design. The additional twist proved to be a significant factor in the turn-on of the TADF relaxation mechanism, ultimately yielding an OLED with an EQE_{max} of 17%.

Furthermore, for the chemical vapor deposition (CVD) process, the influence of molecular chirality on the helicity of polymerized fibers was evaluated. For this suitable chiral [2.2]paracyclophane derivatives were provided and could be shown that chirality can be transferred from the molecular level to a micrometer environment.

Ultimately, the spherical skeleton proved to be a promising guest molecule in supramolecular chemistry when functionalized properly.

During all these synthetic challenges, the peculiarities of this intriguing structure were observed and investigated, leading to the discovery of a unprecedented *para*-selective C–H activation and a synthetic access to the novel (1,7)carbazolophane.

1 Introduction

"*Chemical synthesis is uniquely positioned at the heart of chemistry, the central science, and its impact on our lives and society is all pervasive*."[10] was written by E. J. Corey in his Nobel Lecture in 1991 in order to emphasize the role synthesis has. And G. S. Hammond said that "*The most fundamental and lasting objective of synthesis is not production of new compounds, but production of properties*."[11] To comply with both valid statements, it is fundamental for present-day organic synthesis to selectively plan and carry out projects in order to discover novel properties in both synthesis and material sciences. In this regard, this thesis focused exclusively on the chemistry and application of a structurally exceptional scaffold, namely the [2.2]paracyclophane (**1**).

This compound is one of the most noteworthy and intriguing representatives of the structural class of cyclophanes (Figure 1) for which systematic studies were pioneered by Cram[2] and Hopf.[12]

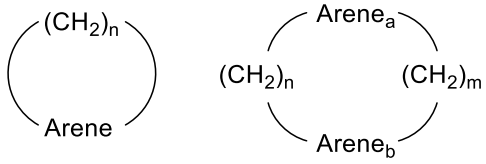

Figure 1. Conceptional representation of the structural class of cyclophanes.

This class consists of a **cycl**ic arrangement of at least one aromatic (**ph**enyl) and at least one aliphatic bridge (alk**ane**) and can therefore include pure hydrocarbon compounds while aliphatic or aromatic heteroatoms are common. In Figure 2, a small selection of remarkable representatives of this structural class is given. Apart from the later discussed [2.2]paracyclophane (**1**), this structural class is ubiquitous in chemistry, e.g. "Stoddart's blue box" (**2**),[13] which is frequently used in supramolecular chemistry to prepare catenanes,[14] or the natural product myricanol(**3**),[15] which can be isolated from *Myrica cerifera* and is used as an anesthetic in folk medicine. Even the Vogel aromatic **4**, a bridged [10]annulene, can be considered a cyclophane.[16]

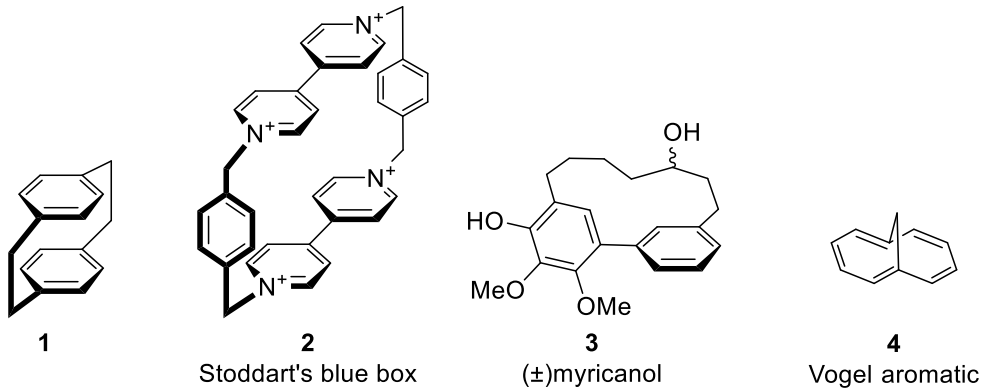

Figure 2. Selected examples of cyclophanes.

In contrast to non-cyclic compounds, the often short bridges in cyclophanes are able to impede or completely prohibit free rotation and therefore can constrain these molecules into unusual and thermodynamically disfavored conformations.[17] The biphenyl bond in compound **3**, for example, is bent out of the planes of both phenyl rings.[15] The investigation of structural peculiarities, and the special chemical properties that derive, represent an exciting field of synthetic chemistry, which also includes propellanes.[18] The archetypical representative of strained cyclophanes is the [2.2]paracyclophane (**1**) which was perfectly paraphrased by Cram as "*bent and battered benzene rings*".[2]

1.1 The [2.2]Paracyclophane

1.1.1 Structure of [2.2]Paracyclophane

First reported by Brown and Farthing,[1] the [2.2]paracyclophane **1** is a strained system with the benzene rings (also called "decks") significantly bent out of the expected ring plane (Figure 3). This is caused by the short ethyl bridges, which force the bridgehead atoms of the benzene rings out of the expected aromatic planarity at an angle of 13°. Additionally, the two stacked rings are declipsed with equilibration observed even at 93 K.[3] The forced boat-shaped structure results in a reduced overlap of the p-orbitals and thus leads to a diminished aromaticity. Furthermore, the distance between the two benzene rings amounts to 3.09 Å, which is 92% of the layer distance reported for graphite (3.35 Å).[19] Therefore, it is commonly accepted that there is interaction between the two π-systems of both benzene moieties. These special properties can be seen in ^{1}H NMR, where the aromatic protons are shifted upfield to δ = 6.50 ppm, while in benzene they are observed at δ = 7.26 ppm.[2-3] The central C–C single bond in the ethylene bridge is 6% longer than "normal" single bonds.[20] The ring strain amounts to 134 kJ/mol, and rotation of the benzene units is not possible due to the short bridges. This conformational stability allows the synthesis and separation of enantiopure derivatives.[21] All these structural abnormalities correlate with peculiar chemical properties.

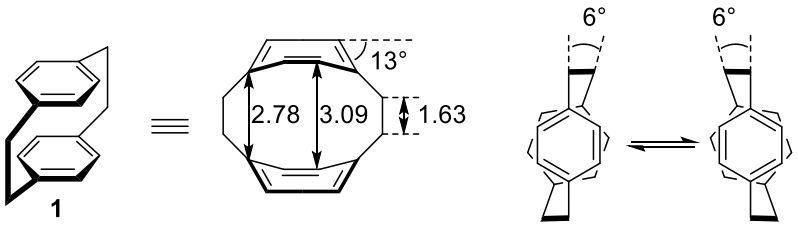

Figure 3. Structural parameters of [2.2]paracyclophane. Distances are given in Ångström.[22]

Since naming of cyclic compounds is rather difficult, the official IUPAC nomenclature for cyclophanes is inconvenient. Therefore, Vögtle *et al*. developed a specific cyclophane nomenclature, which is based on a core-substituent ranking.[23] The core structure is named according to the length of the aliphatic bridges in square brackets (e.g. [n.m]) and the benzene substitution patterns (*ortho*, *meta* or *para*).

[2.2]Paracyclophane belongs to the D_{2h} point group, which is broken by the first substituent, resulting in two planar chiral enantiomers. By definition, the arene bearing the substituent is set to a chirality plane (Figure 4, top), and the first atom of the cyclophane structure outside the plane and closest to the chirality center is defined as the "*pilot atom*". If both arenes are substituted, then the substituent with higher priority according to the Cahn-Ingold-Prelog (CIP) nomenclature is preferred.[24] The stereodescriptor is determined by the sense of rotation viewed from that pilot atom and to indicate the planarity of the chiral center, a subscripted *p* is added.[25]. To correctly describe the positions of the substituents, an unambiguous numeration is needed, but unfortunately, the numbering of the second arene is not consistent in literature. The numbering of the arenes should follow the sense of rotation determined by CIP, but another description based on the benzene substitution patterns is preferred for disubstituted [2.2]paracyclophanes, (Figure 4, bottom) with the descriptor "pseudo" when the substituent is at the second arene.

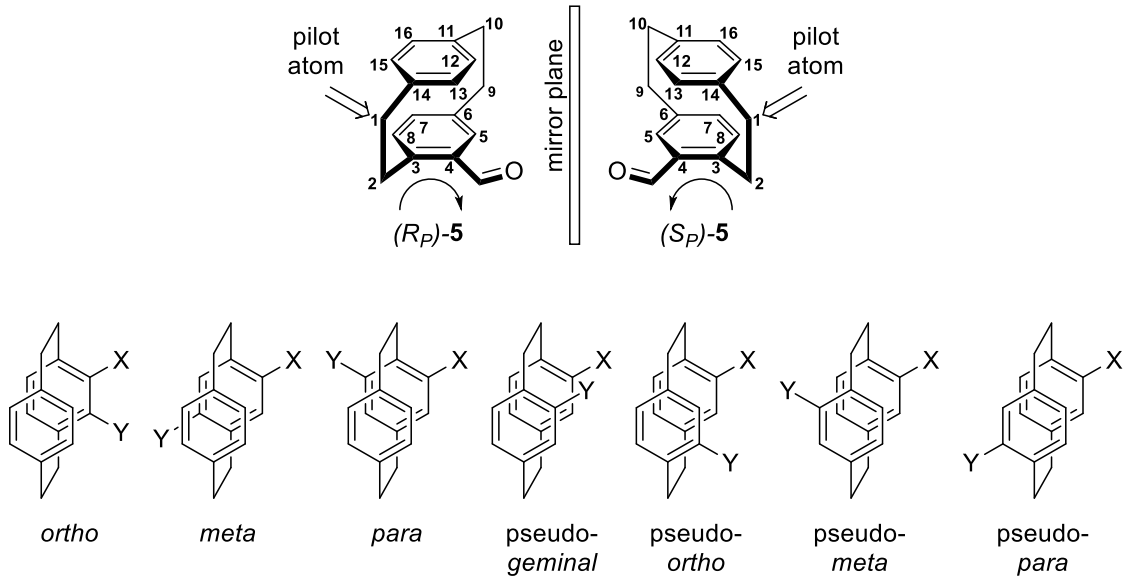

Figure 4. Top: Nomenclature and chirality descriptors exemplified by 4-formyl[2.2]paracyclophane (**5**). Bottom: Available aromatic substitution pattern of disubstituted [2.2]paracyclophane with relative nomenclature.

1.1.2 Synthesis of [2.2]Paracyclophane

The first synthesis of [2.2]paracyclophane was carried out in 1948 by Szwarc during pyrolytic studies of C–H bond energies of xylenes without further investigation of the products formed,[26] which was done one year later by Brown and Farthing.[1] Nevertheless Szwarc proposed that the comparatively fast decomposition of *p*-xylene (**6**) yields a quinodimethane diradical species **7** (Scheme 1), that can either dimerize to give [2.2]paracyclophane (**1**) or form polymers. As indicated, this process is in principle reversible.

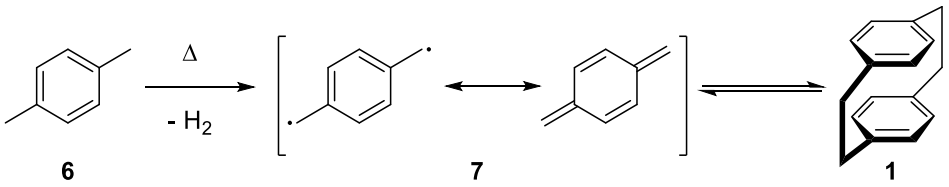

Scheme 1. Pyrolysis of *p*-xylene (**6**) to the quinodimetane (**7**) intermediate, which dimerizes to yield [2.2]paracyclophane (**1**).

In 1951, Cram *et al.* began thorough research on the aromatic anomalies, which strained macrocyclic compounds exhibit. Therefore, a general method was developed to access [n.m]paracyclophanes by intramolecular Wurtz coupling (Scheme 2).[27]

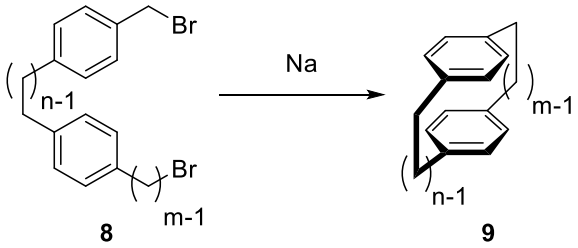

Scheme 2. First targeted synthetic access to [n.m]paracyclophanes **9** including the [2.2]-representative **1** by Cram *et al.*[27]

Another route uses the quinodimethane intermediate **7** generated *via* 1,6-Hofmann elimination (Scheme 3) of suitable precursors such as **10** which undergoes dimerization under less harsh conditions to yield the desired [2.2]paracyclophane (**1**).[28-29]

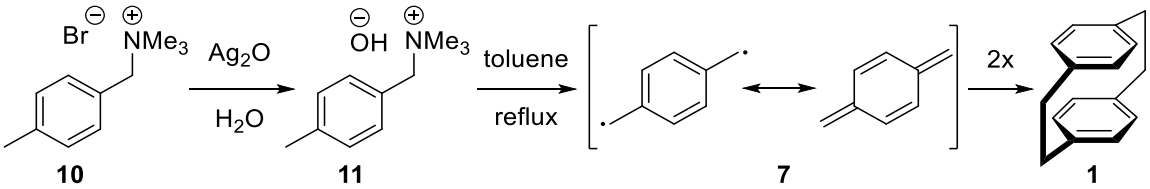

Scheme 3. 1,6-Hofmann elimination generates quinodimethane intermediate **7** to access [2.2]paracyclophane (**1**).[28]

A further approach employs the [3.3]dithiacyclophane **14** which can be easily prepared from the dithiol **12** and the dibromide **13**. This larger cyclophane undergoes ring contraction *via* sulfur extrusion through Pummerer,[30] or Stevens rearrangement.[31] This particularly elegant method is extraordinarily suitable to access [2.2]paracyclophanes with functionalizations at the aliphatic ethyl bridges, which are key intermediates to [2.2]paracyclophane-1,9-diene,[30] or to access disparately substituted phane decks, such as the [2.2]pyridinophane, which exhibits one benzene and one pyridine unit.[32]

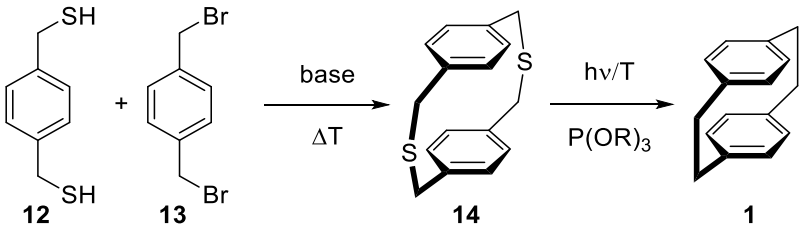

Scheme 4. Access to [2.2]paracyclophane (**1**) *via* sulfur extrusion of [3.3]dithiacyclophane **14**.

1.1.3 Reactivity of [2.2]Paracyclophane

1.1.3.1 Initial Functionalization

As an aromatic compound, [2.2]paracyclophane (**1**) is readily functionalized by electrophilic aromatic substitution reactions (Scheme 5), such as nitration, acylation, formylation and bromination, which give access to initial functionalized derivatives in good yields.

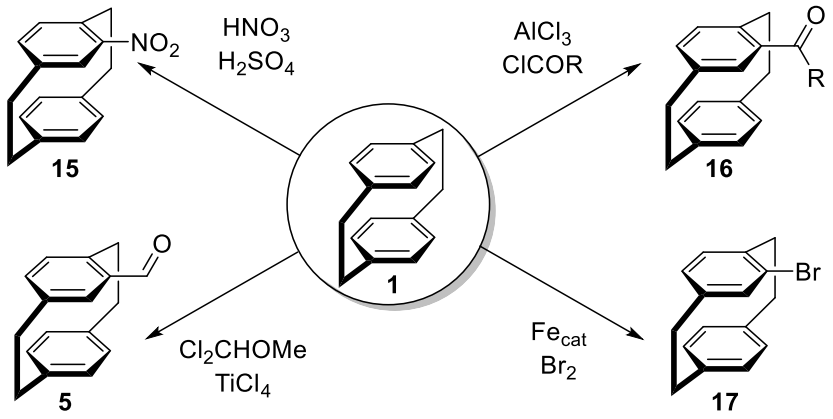

Scheme 5. Initial functionalization strategies in [2.2]paracyclophane chemistry.[33]

Due to the close vicinity of the benzene rings, a transannular directing effect for a second functionalization *via* electrophilic aromatic substitution (S_NAr) is observed with structural carbonyl groups such as ketones, esters, amides, oxazolines, phosphine oxides, sulfones, sulfoxides and nitro groups. The substitution occurs at the pseudo-*geminal* position with nearly exclusive selectivity and can be explained by evaluation of the mechanism (Scheme 6). During S_NAr, the π-complex **18** is formed a-top the electron-rich benzene ring. In case of the mentioned functional groups, this is always the non-functionalized ring. This η^6-complex selectively collapses to the σ-complex **19** (Wheland intermediate), because the *ipso*-hydrogen stands pseudo-*geminal* to the carbonyl function and is therefore readily deprotonated to give the intermediate **20**.

1.1.3.2 Strategies Towards Difunctionalized Derivatives

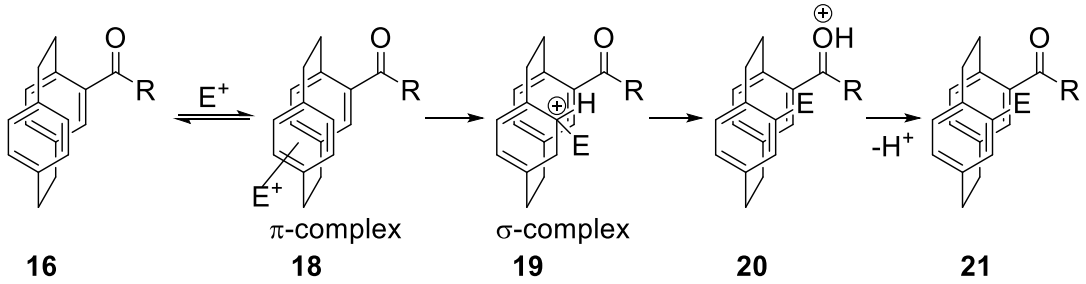

Scheme 6. Transannular directive effect of carbonyl structural groups to pseudo-*geminal* selective second functionalization *via* electrophilic aromatic substitution.[33]

Furthermore, bromination can be performed numerous times to yield dibromo[2.2]paracyclophanes, but does yield a mixture of different-pseudo-dibrominated isomers, which require tedious separation (Scheme 7).[34] The centrosymmetric pseudo-*para* dibromide **22** can be easily separated from the remaining mixture of isomers due to its low solubility and is therefore a well-used intermediate to difcunctionalized derivatives. Optimized reaction conditions lead to a 34% yield of **22**.[33]

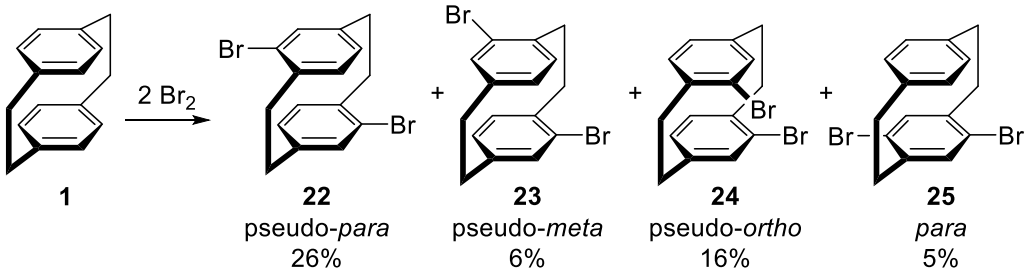

Scheme 7. Dibromination of [2.2]paracyclophane with isolated yields reported by Cram *et al*.[34]

In contrast to the iron catalyzed or non-catalyzed access to aromatic bromide **17** or **22**–**25**, functionalization at the aliphatic ethyl bridges can be achieved by photochemically initiated bromination (Scheme 8). De Meijere *et al.* reported tetrabromination to yield a mixture of 1,1,9,9- and 1,1,10,10-tetrabromides **26** and **27**.[35]

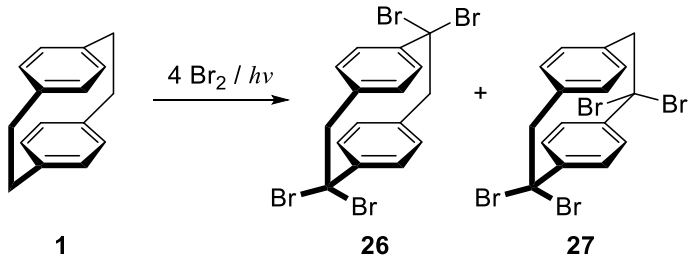

Scheme 8. Aliphatic bromination under photochemical conditions.[35]

The afore mentioned synthetic access *via* dimerization of quinodimethane intermediate **7** is reversible as ring strain is released, but this process occurs *via* a two-step mechanism where both tethers of the

[2.2]paracyclophane are opened homolytically in a sequential manner at high temperatures. By carefully tuning the reaction temperature, this mechanism can be set to hold at one broken ethyl bridge yielding a non-cyclic and therefore non-strained diradical, which is able to recyclize. This property is commonly exploited for the synthesis of pseudo-*ortho* dibromide **24** from the readily available pseudo-*para* dibromide **22** (Scheme 9). Despite this potential decomposition pathway of [2.2]paracyclophanes, the thermal isomerization proceeds only at significantly elevated temperatures of 200 °C.

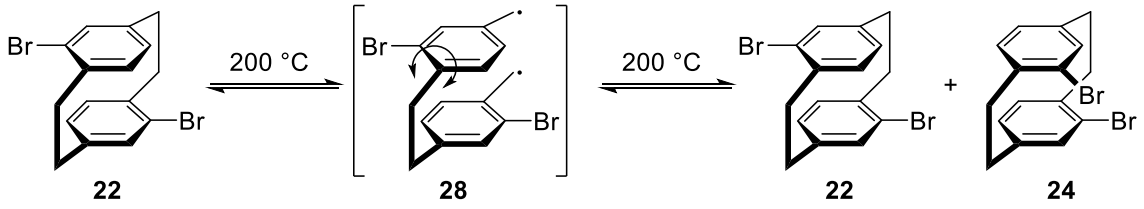

Scheme 9. Thermic isomerization of the [2.2]paracyclophane backbone leads to differently substituted stereoisomers.[33]

Further access to *ortho*-functionalized derivatives can be obtained by templated lithiation. As an example from Pelter *et al.* (Scheme 10),[36] the amide **30** can lead to both the pseudo-*geminal* bromide **31** *via* the previously discussed transannular directing effect or to the *ortho*-bromide **29** by templated lithiation.

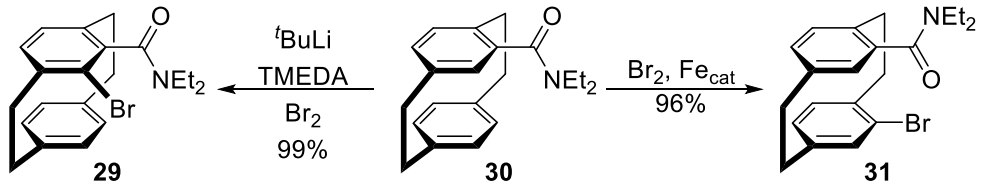

Scheme 10. Choice of regioselectivity for amide **30** can be set by selected reaction protocols (electrophilic substitution *versus* lithiation).[36]

With regard to synthetic strategies to difunctionalized [2.2]paracyclophane derivatives, pseudo-*geminal* and pseudo-*para* substitution patterns can be readily accessed by pseudo-*geminal* directive effects, and by easy separation of the dibromide **22**, respectively. The pseudo-*ortho* substitution pattern can be obtained using the dibromide **24** and *ortho*-functionalization is attained by directed lithiation.

In contrast pseudo-*meta*, *meta* and *para* substitution patterns are much more challenging to obtain, and are often accessed *via de-novo* syntheses of the whole [2.2]paracyclophane skeleton.

1.1.4 C–H Activation

C–H activation on the [2.2]paracyclophane structure was first explored by Bolm *et al*. starting in 2012. It was shown that *ortho*-selective acetoxylation mediated by $Pd(OAc)_2$/PIDA can be effectively directed by aldoxime ethers, ketoxime ethers and esters, 2'-pyridyl and pyrazole directing groups (Scheme 11) in good yields and selectivity under acidic conditions.[37]

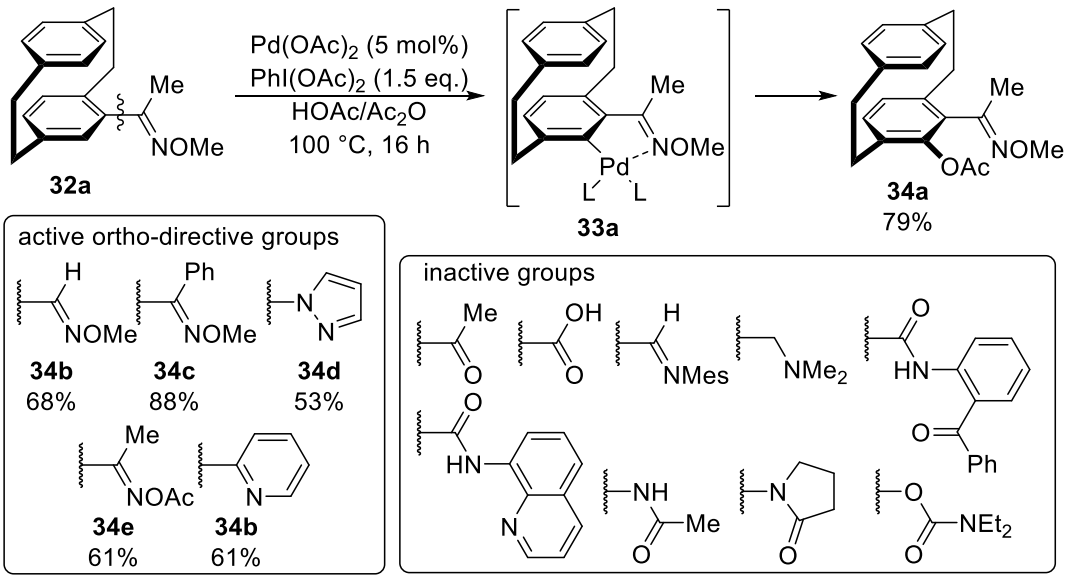

Scheme 11. Overview of performance of directive groups in *ortho*-C–H activation from Bolm *et al*.[37]

Although oximes proved to be excellent *ortho*-directing groups for Pd-catalyzed *ortho*-C–H activation, numerous other common directing groups were inactive, either because they were incompatible under the reaction conditions or too bulky.

Related to these findings, a Pd-catalyzed *ortho*-bromination/iodination procedure was described presenting a swifter access to *ortho*-functionalized intermediates although 20 mol% catalyst loading was needed to obtain 63% of products **35** (Scheme 12).[38]

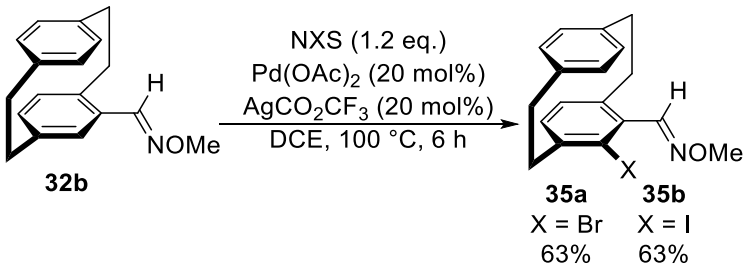

Scheme 12. Pd-catalyzed *ortho*-bromination. [38]

Bolm *et al.* further used their procedure of *ortho*-C–H activation under acidic conditions to synthesize (1,4)-bridged carbazolophanes **37** (Scheme 13) *via* oxidative cyclization under aerated conditions starting from *N*-phenylamino[2.2]paracyclophane **36**.[39] In contrast to the *ortho*-acetoxylation, a significantly increased catalyst loading of 20 mol% is needed to obtain **37** in 62% yield. Interestingly,

the oxidative cyclization does not occur with a *N*-methylated derivative of **36**. Although the reaction conditions are rather harsh, this protocol is reported for a wide range of electron-rich and -poor aniline derivatives. This gives access to a very interesting class of planar chiral (1,4)-bridged carbazolophanes which are suitable for material sciences as they both exhibit an increased steric demand and planar chirality.

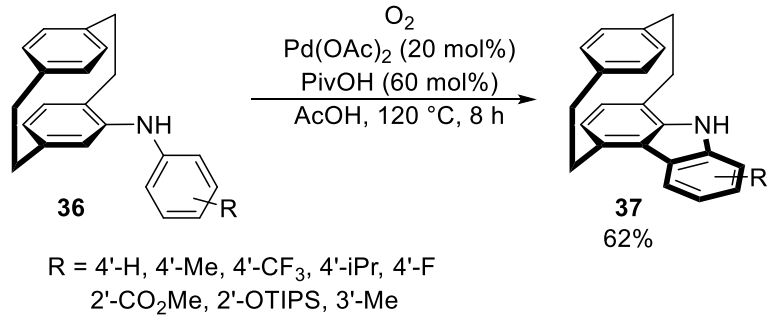

Scheme 13. Oxidative cyclization in *ortho*-position to planar chiral (1,4)-bridged carbazolophanes.[39]

1.1.5 *para*–Activation

Bolm *et al.* also reported a *para*-functionalization of phenylamino, acetamido (and derivatives)-substituted [2.2]paracyclophanes (e.g. **38**). To obtain the product **39**, phenyliodide diacetate (PIDA) was used as the oxidant to mediate the addition of various nucleophiles (Scheme 14). Nucleophiles such as acetate, formate, methanolate, ethanolate and bromide can be successfully attached at the *para*-position in moderate to good yields. An insight into the mechanism was given, when an excess of PIDA was added, which led to the mixed benzoquinone **40** in 54% yield.[40]

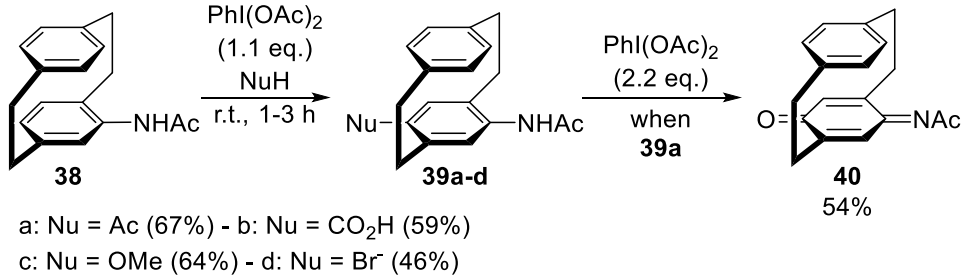

Scheme 14. PIDA mediated *para*-functionalization and formation of side product **40** when an excess of oxidant is used.

In a related manner, benzoquinone **43** was reported by Cram already in 1966. It is a convenient intermediate,[41-42] since both, the precursor **41** is available, and the benzoquinone **43** can be readily converted to a *para*-bistriflate **44**,[43] suitable for cross-coupling.[44]

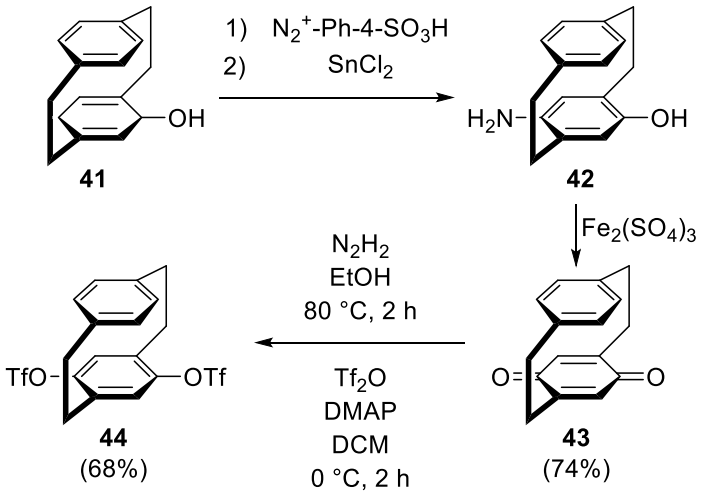

Scheme 15. Oxidative *para*-functionalization with benzoquinone intermediates.

Finally, *para*-bromination was reported for the methoxy derivative **45** in 86% yield but has not gained much attention due to the stability of a methoxy functional group with regard to further derivatization.[45]

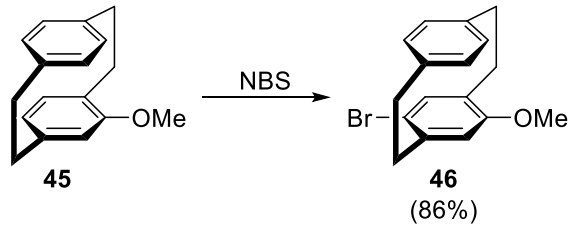

Scheme 16. Direct *para*-bromination of activated 4-methoxy[2.2]paracyclophane (**45**).[45]

1.1.6 Chiral Resolution

Separation of planar chiral derivatives of [2.2]paracyclophane can be a tedious endeavor, especially on a large scale. In order to circumvent expensive chiral (semi)preparative HPLC techniques, chiral resolution *via* derivatizing agents has been reported in some cases. Racemic 4-formyl[2.2]paracyclophane **5** can be easily enantioenriched by repeated fractional crystallization of the diastereomeric mixture of imines **48** (Scheme 17).[46-48] The enantiomerically and diastereomerically pure imine is easily hydrolyzed on silica, yielding (S_P)-**5** in excellent enantiomeric purity. Although only the (S_P) isomer is isolated when using the (*R*)-amine **47**, it is possible to obtain the other enantiomer, when (*S*)-**47** is used. The enantiomeric excess is conventiently monitored by ^{1}H NMR of the imine proton. This procedure has proven successful also for an *ortho*-hydroxy-formyl-[2.2]paracyclophane derivative.[47]

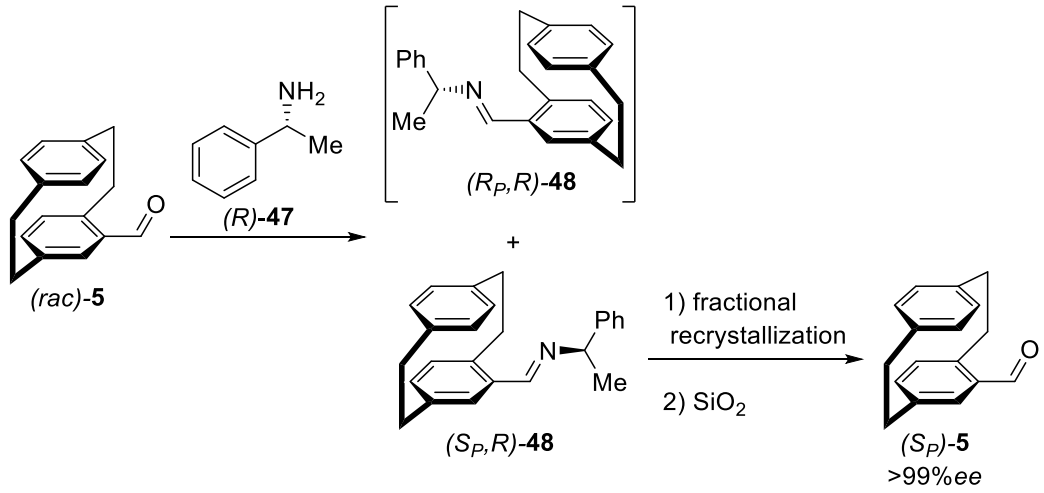

Scheme 17. Chiral resolution of 4-formyl[2.2]paracyclophane **5**.

Ultimately, Rowlands *et al.* reported chiral sulfoxides **51** prepared from thiosulfinate **49**[49] and toluenesulfinate **50**[50] as suitable derivatizing agents for the [2.2]paracyclophane core which can be separated by column chromatography on a 10 gram scale (Scheme 18)[51] with >99%*ee* when **51b** is used.[50] The sulfoxide group can be cleaved by addition of *n*-butyllithium to obtain an enantiopure **Li-52** reactive intermediate which can be conveniently quenched with a number of electrophiles,[49] or can be derivatized to a chiral thiol,[52] essentially promising a single methodology to access a wide range of precursors in an enantiopure way. Furthermore, these chiral sulfoxides are able to direct further functionalization to the *ortho*-position *via* lithiation[49] or pseudo-*geminal* position *via* electrophilic bromination.[53]

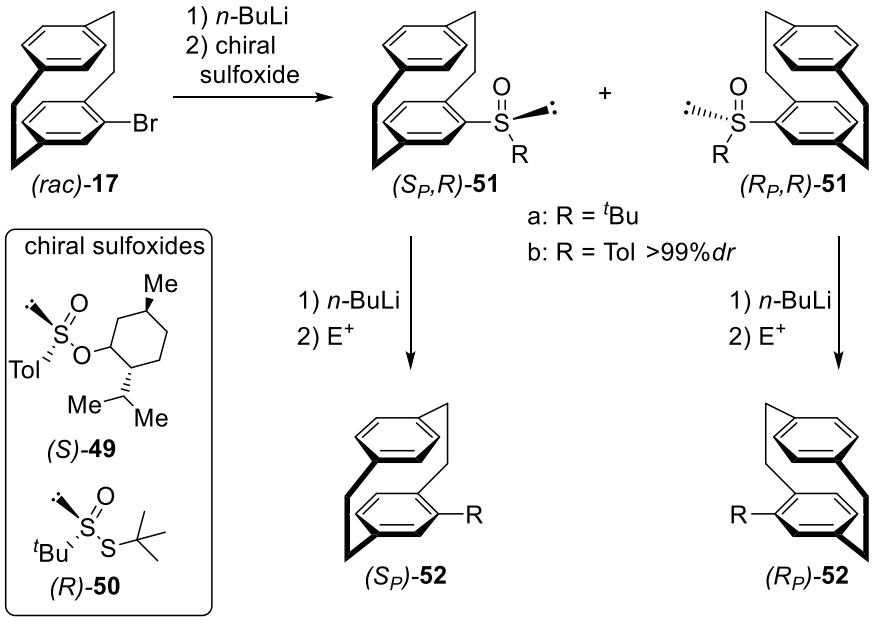

Scheme 18. Chiral resolution *via* chiral sulfoxides explored by Rowlands *et al.*[51]

1.1.7 Unprecedented Rearrangements

Due to the structural peculiarities of the [2.2]paracyclophane, this molecule is prone to unexpected reactivity. For instance, a shift of the ethyl bridge has been observed upon addition to the quaternary bridgehead carbon.

The first reported example was observed during a Fischer-type indole synthesis with ethyl pyruvate (**54**) leading to the ene-hydrazine starting material **55** (Scheme 19). An unselective addition to either the quaternary (**56**) or primary (**58**) *ortho*-carbon was observed, which led to the expected fused (4,7)-bridged indolophane **57** in 23% yield and the novel (3,6)-bridged indolophane **59** in identical yield caused by a [1,2]-shift of the ethyl bridge.[54] Even though alkyl-shifts can occur in Fischer-type syntheses,[55] this behavior was only observed when using ethyl pyruvate (**54**) to generate **55**. No such side product was observed when using cyclohexanone and butanone to generate the respective derivatives of **55**. This is explained by an improved enamization of **55** caused by the carboxyethyl group.

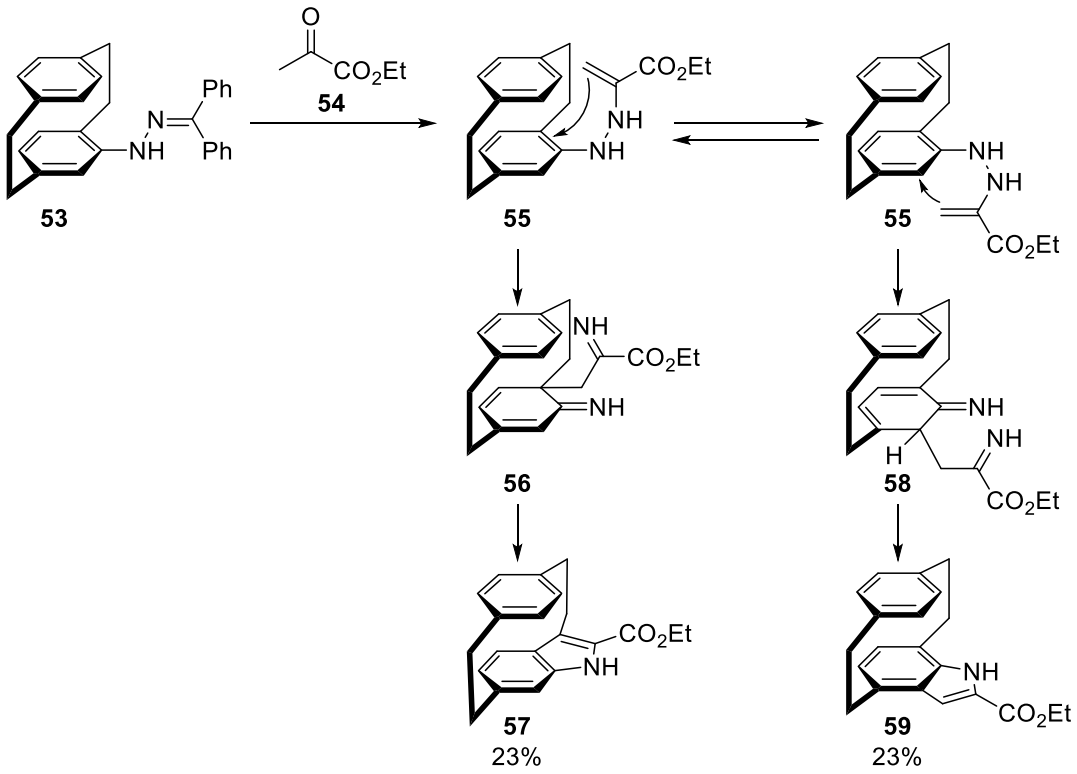

Scheme 19. Fischer-type indole synthesis on [2.2]paracyclophane yielding both typical and atypical indoles **59** and **57**.

A second example for the reactivity of the quaternary bridge-head carbon was observed during a Gould-Jacobs synthesis to access 4-quinolones from the cumulene intermediate **61**.[56] Here, a thermally generated cumulene **61** from decomposition of the malonic enamine precursor **60** proved to generate the expected (5,8)-bridged cyclophane **63** and the unexpected (3,7)-bridged cyclophane **65** in equal amounts. Again a very similar mechanism was proposed starting from a rotamer leading to the addition to the quaternary carbon giving intermediate **64**, which undergoes a subsequent [1,3]-shift.

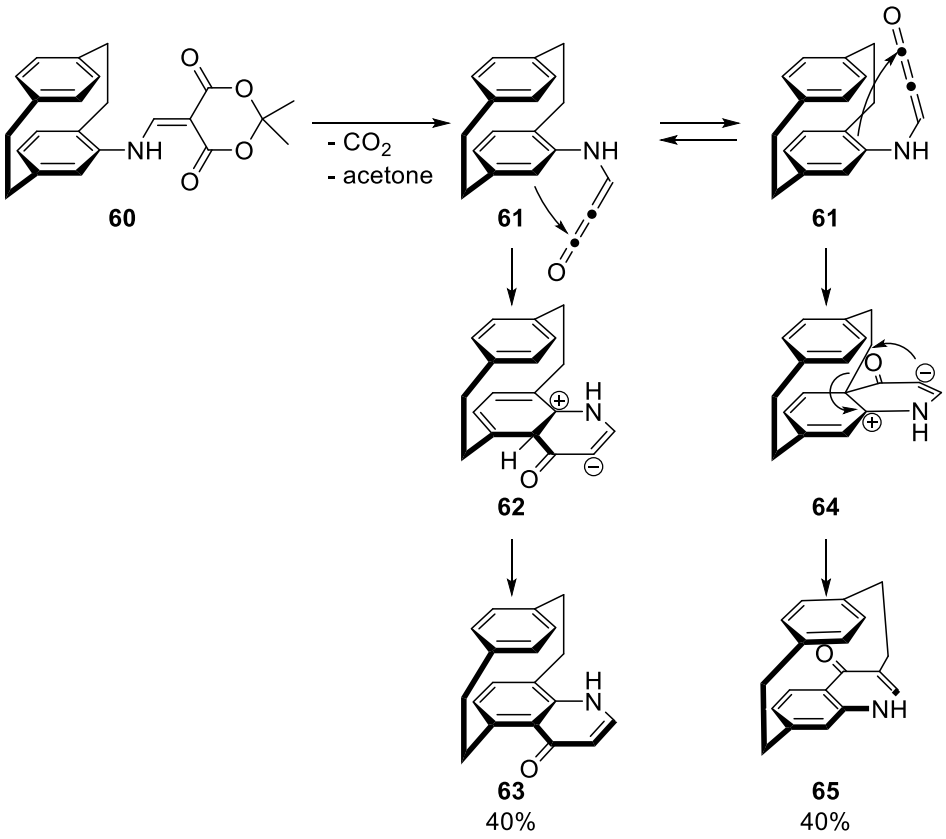

Scheme 20. Gould-Jacobs synthesis of the expected 4-quinolonophane **63** and the unexpected **65**.

In both examples it must be noted, that the isolated yields of the desired and unexpected products were equivalent, essentially demonstrating that there is no selectivity between the primary and quaternary position under the reported conditions. The reactivity of the quaternary carbon under relatively harsh conditions has not been systematically investigated so far, but can give access to a wider range of (hetero)aromatic cyclophanes with short ethyl bridges.

1.2 Chemical Vapor Deposition Polymerization[1]

1.2.1 Concept

First described by Gorham in 1966, [57] [2.2]paracyclophane can be cracked homolytically at the ethylene bridges at high temperatures yielding 1,4-quinodimethanes in gas phase (Scheme 21). In principle this is the reverse process of the [2.2]paracyclophane synthesis described previously in section 1.1.2. The potential of this process was first explored by Gorham in 1966.[57] Under suitable reaction conditions the 1,4-quinodimethane diradicals recombine in a polymeric fashion rather than reform the rigid [2.2]paracyclophane scaffold. Polymer coated surfaces are obtained, indicating that the diradicals in gasphase deposit on the surface prior to recombination. Therefore, this process is coined chemical vapor deposition (CVD) polymerization. The poly-*p*-xylylenes (PPX) coatings are generally referred to as parylenes. With a suitable device setup and by a carefully tuned gas flux under reduced pressure, CVD can be performed on any object,[58] enabling a generic surface engineering protocol. Although the [2.2]paracyclophane scaffold is cracked under pyrolytic conditions (> 550 °C), numerous functional groups survive this step, tremendously increasing the potential for post-CVD surface engineering, as well.

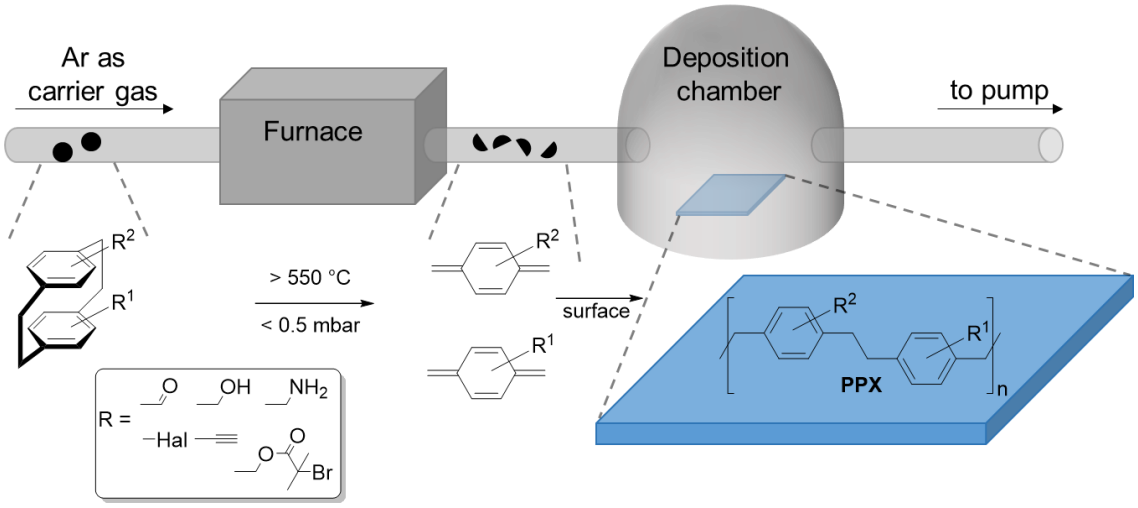

Scheme 21. Mechanism and system setup of chemical vapor deposition (CVD) polymerization.

By a reasonably sophisticated system setup with e.g., numerous pyrolysis chambers or a patterning mask and sequential deposition of different precursors, random copolymers, gradients[59] and microstructuring can be obtained.

This CVD process is especially useful for medical and biological applications as no side products are generated in the homolytic σ-bond dissociation when compared to the alternative access to parylene coatings *via* 1,6-elimination of e.g. chloro-methyl *para*-xylenes yielding hydrochloric acid as a side

[1] Parts of this chapter have been published in:
Z. Hassan, E. Spuling, D. M. Knoll, J. Lahann, S. Bräse, *Chem Soc. Rev.* **2018**, *47*, 6947–6963.

product. Although the polymers obtained are not chemically bound to the surface, their high molecular weight and high degree of aromaticity result in mechanically stable (tape test)[60] coatings and often inhibits further characterization due to a lack of solubility. In this regard alkyl substituted [2.2]paracyclophanes were prepared by Greiner and coworkers to permit characterization.[61] The results showed a randomly distributed head to tail selectivity, polymers with a number average of up to 258 000 Da and a polydispersity in the range of 2.6 to 4.5. Although further fundamental research of the Gorham process is still pending the CVD of functionalized [2.2]paracyclophanes yields numerous parylene coatings with intriguing properties and potential applications.

1.2.2 Applications

The chemical inertness and low permittivity make parylenes widely used for coatings of electrical[62] and medical devices.[63-64] The wide range ofapplications of this process is evaluated, amongst others, by Lahann and coworkers in numerous examples, such as orthogonal immobilization of two different biomolecules by amide formation with surface deposited methylamino groups and Huisgen click reaction to surface deposited terminal alkynes,[65] a pH dependent swelling of the coating when methylamino groups are deposited,[66] and the formation of a backbone degradable polyester copolymer by gas phase ring-opening rearrangement of a cyclic ketene acetal (Scheme 22 top).[67]

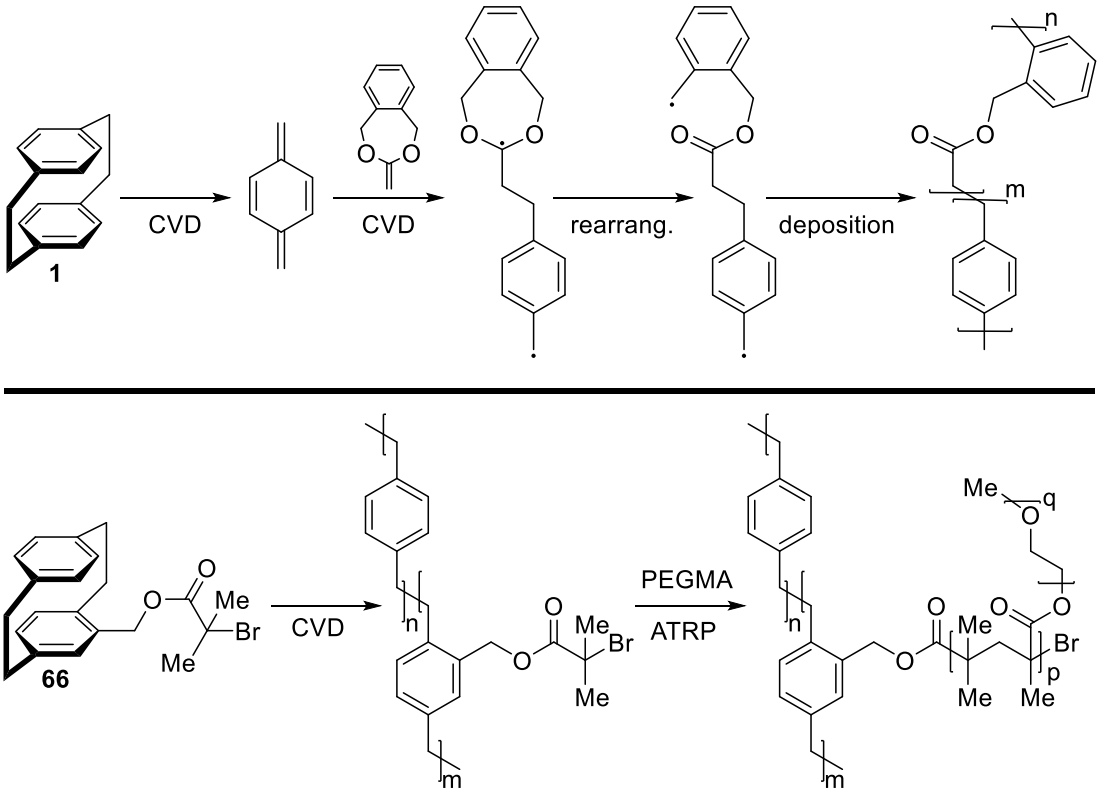

Scheme 22. Top: CVD synthesis of biodegradable parylene copolymers.[67] Bottom: CVD deposition of 2-bromo propyl functionalities gives access to reactive coatings suitable for ATRP polymerization.[68]

In the context of reactive coatings for post CVD functionalization, it has been shown that a suitable ATRP initiator **66** was successfully deposited on surface, enabling a surface-bound yet substrate independent polymerization which was demonstrated with PEGMA (poly(ethylene glycol) methacrylate) in order to obtain bioinert surfaces (Scheme 22 bottom).[68]

Furthermore, CVD was also performed with functional pyridinophane derivatives such as **67** (Scheme 23). In this case polylutidin-co-polyxylylene copolymers were obtained. These polymers show an increased adhesion of HUVEC cells due to the increased polarity and hydophilicity of the material through the incorporated nitrogen.[32] In case of the unsubstituted pyridinophane and the *para*-alkynyl derivative, a patterning and post CVD functionalization was demonstrated by Huisgen click methodology of azido biotin and subsequent incubation with fluorescent streptavidin.

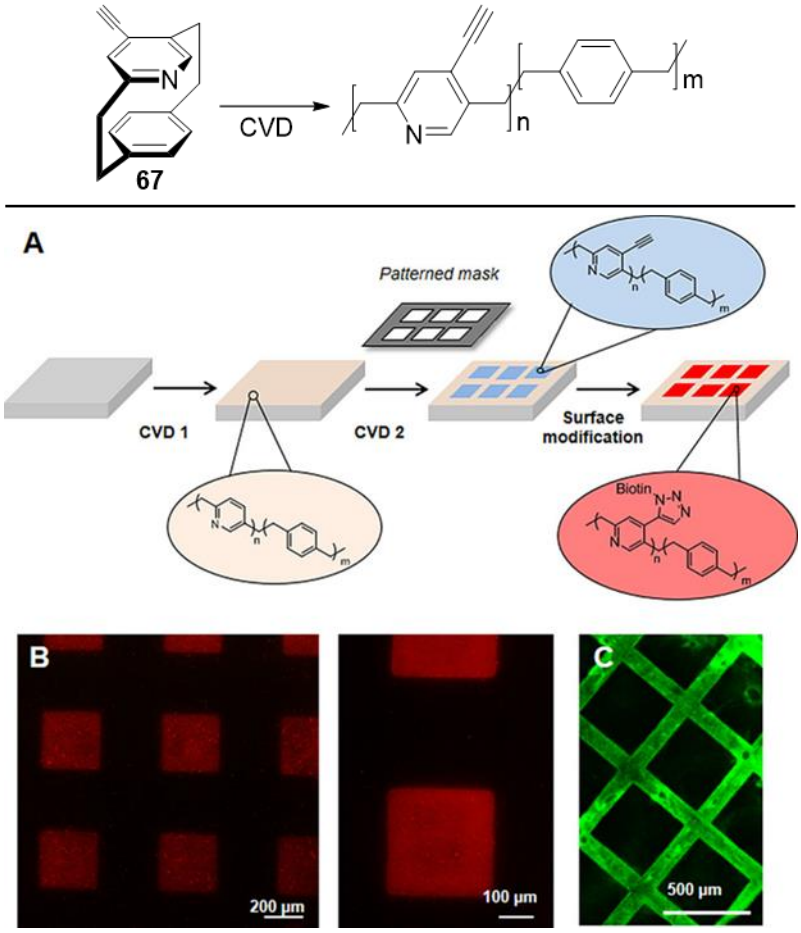

Scheme 23. Top: Formation of functional polylutidine-co-parylene polymers. Bottom: A) Schematic representation and B,C) Demonstration of micropatterning and post CVD functionalization. Reprinted with permission from *Chem. Eur. J.* **2017**, *23*, 13342–13350.[32]

Recently, Lahann *et al.* presented a templated CVD protocol. By using anisotropic liquid crystals (LC), surface anchored nanofibers could be synthesized as schown in Scheme 24.[69] Most notably, by using nematic liquid crystals, linear fibers were obtained, while blue-phase liquid crystals yielded nanostructures with pores of around 500 nm in diameter. For this thesis most relevant is the observation

that by using cholesteric liquid crystals, the helical chirality could be reliably transferred to the obtained nanofiber in the form of a spiraling of the fiber in the µm range. Evaluation of adhesion forces clearly showed that interlocking of fibers increases the adhesion force when compared to nontemplated parylene coated surfaces. Additionally, an influence of the relative chirality of two cholesterically templated nanofibers on the adhesion force is observed.

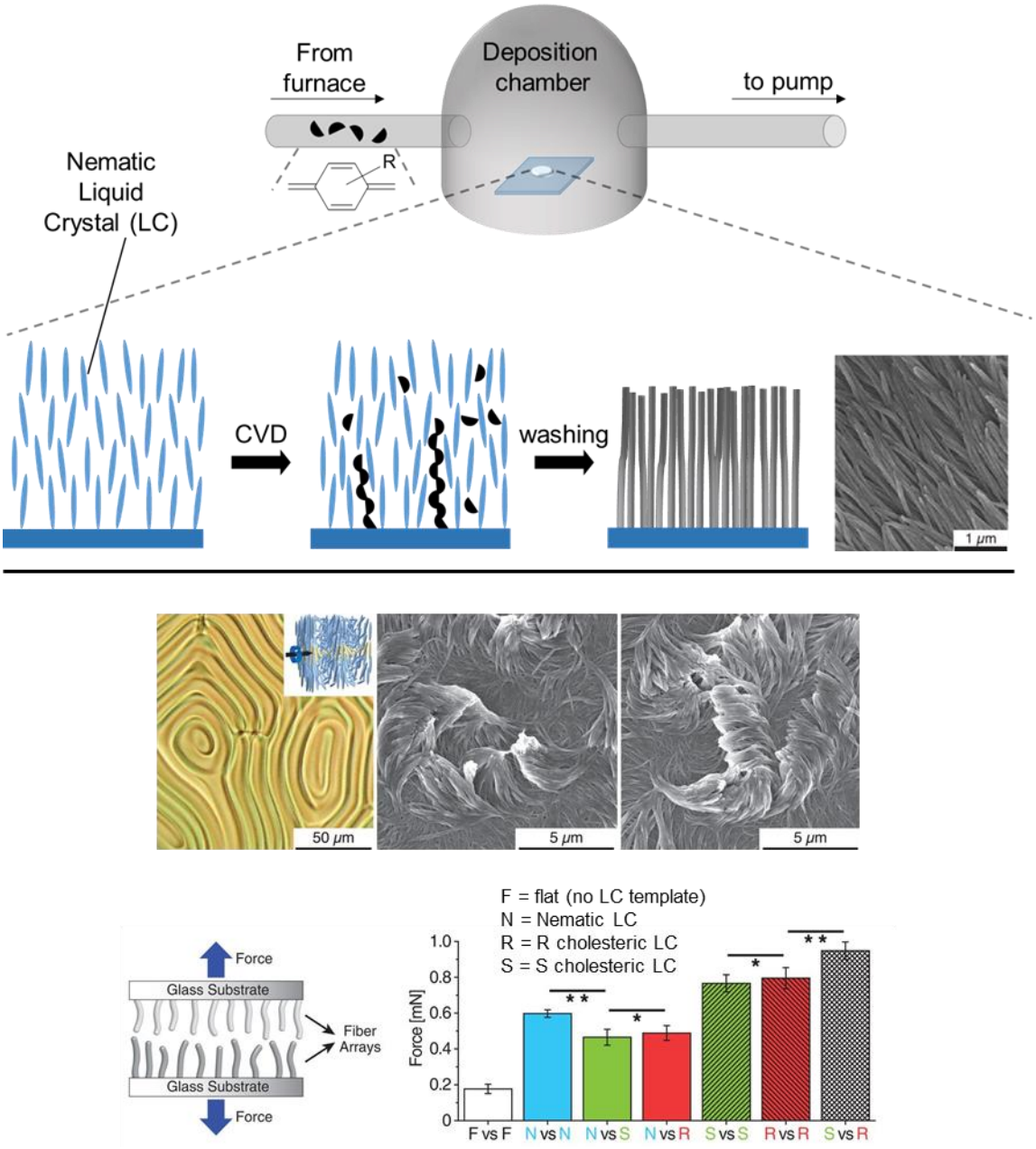

Scheme 24. Top: Concept of liquid crystal (LC) templated CVD polymerization of nanofibers. SEM images of nanofibers. Bottom: Cholesterically templated helical nanofibers with evaluation of adhesion forces. Parts reprinted with permission from *Science* **2018**, *362*, 804–808.[69]

1.3 TADF and OLED

In order to understand the thermally activated delayed fluorescence (TADF) mechanism, and its value for modern light harvesting, the principles of an organic light-emitting diode (OLED) will now be introduced.

1.3.1 Organic Light-Emitting Diodes (OLEDs)

Organic light-emitting diodes are carefully manufactured devices designed to generate light through electroluminescence. This property was first described by Bernanose *et al.* in 1955 by measuring a mixture of phosphorescent organic dyes in an inert polymer matrix placed in a dielectric cell.[70] Investigation of the basic mechanism only started after this phenomenon was observed on anthracene crystals by Pope *et al.* in the early 1963.[71-72] The break through report was made in 1987 by Tang and van Slyke who prepared the first dedicated OLED device with an external quantum efficiency of 1% and a brightness of 1000 cd m^{-2} at a driving voltage below 10 V.[73] Therefore, 8-hydroxyquinoline aluminum (Alq_3) was deposited in a layered device architecture by vapor deposition, which generated green light (550 nm). The discovery of metal-like conductivity of redox doped polymers by Heeger *et al.*, who were honored with the Nobel Prize in Chemistry in 2000, finally started the industrial development of OLEDs.[74]

Compared to inorganic LEDs, OLEDs offer solution-based processability and the avoidance of precious elements. This promises an inexpensive and a more environmentally friendly fabrication. Furthermore, as the only available planar light source, which can be fabricated onto flexible and transparent substrates, novel design concepts are accessible.

1.3.1.1 Architecture and Functionality of OLEDs

The elementary processes of an OLED device are described in Figure 5. In the first step (I), charge carriers are injected into the organic materials of the OLED device through the cathode and anode. The induced electric field slopes the molecular orbitals. To avoid a spontaneous current flow, it is important that the lowest HOMO is lower than the anode, whereas the highest LUMO needs to be higher than the cathode.[75] Next (step II) the injected charges migrate to their corresponding electrode. As molecules exhibit distinct molecular orbitals rather than extensive valence or conduction bands, used to describe inorganic solid-state matter, the migration of charges is seen as a cascade of redox reactions. This results in a hopping mechanism.[76] The efficiency of conductivity is proportional to the distance, temperature, conformational stability between the reduced and oxidized state and the overlapping of orbitals. Hence π-stacking is an important material property for efficient conductivity in OLEDs.[77] Furthermore, extensively conjugated π-systems are preferred as a decreased energy gap between HOMO and LUMO is obtained.[78] In the third step (III), the migrating positive and negative charges recombine to form so called excitons or excited states located at specific molecules. These molecular excited states undergo

relaxation *via* different pathways, of which photoemission (step IV) is the desired process. This process of electrical excitation which relaxes back to the ground state *via* emission of photons is called electroluminescence.[79] The photophysical mechanisms are discussed indepth in the following section 1.3.1.2.

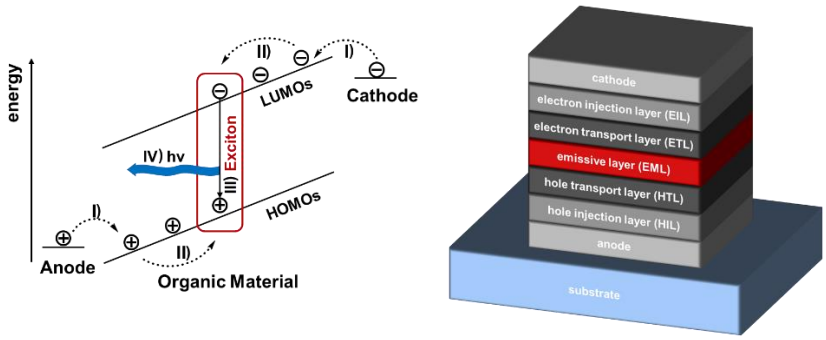

Figure 5. Left) Elementary steps in an OLED device. I) Injection of charge carriers; II) Transport of charge carriers; III) Exciton formation; IV) Light emission. Right) Generalized architectural build-up of OLEDs.

The actual build-up of an OLED device in order obtain a most efficient generation of light is quite sophisticated, as numerous layers need to exhibit distinct features in order to facilitate the charge migration and increase accumulation at the emissive layer. A generalized OLED architecture is presented in Figure 5. The respective purposes are charge injection from the corresponding electrodes, charge transport and blocking and out-coupling of the generated light.[80] The key characteristics of the layer materials are their HOMO or LUMO levels which smoothen the charge transport towards the final emissive layer (EML).

Substrate

In principle the substrate is only needed as the carrier material for the whole OLED architecture. In order to out-couple light, this layer needs to be transparent and depending on the application it can also be flexible. Therefore glass, or transparent polymers are used.[75]

Anode and Hole Injection Layer (HIL)

As cathodes are made of base metals or alloys which are opaque, the anode has to be transparent to allow the outcoupling of light. Indium tin oxide (ITO) $(In_2O_3)_{0.9}(SnO_2)_{0.1}$ has been established as the standard material for this purpose. To avoid indium, other transparent conductive oxides (TCO),[81] or purely organic anodes are explored.[82] As the interfaces of the anode layers are typically rough, a smoothening hole injection layer (HIL) is often deposited on top to level them. Furthermore, the transfer to the following hole transport layer (HTL) can be disposed.

The HIL material must have an electron affinity in the range between the anode and the following layer alleviating the hopping mechanism of the cationic charges *via* HOMOs.[75] The so called PEDOT:PSS

material is commonly used for this purpose. It is a mixture of a conjugated polythiophen polymer and a sulfonic acid derivative of polystyrene.

Hole Transport Layer (HTL) / Electron Blocking Layer (EBL)

The purpose of the HTL is to guide and smoothen the transport of positive charges *via* HOMOs towards the final emissive layer (EML). Additionally, since the charges need to be accumulated within the emissive layer, this layer functions as an electron blocking layer (EBL) for the anionic charges migrating from the cathode. These properties are realized by electron rich heteroaromatic compounds.[75]

Emissive Layer (EML)

In the emissive layer, the charges meet to form excitons. This recombination of opposite charges has to be even to avoid a build-up of charge, as this would induce detrimental and irreversible redox reactions within the material. This layer is doped with electroluminescent emitters, which are responsible to the generation of light *via* photophysical processes discussed below in section 1.3.1.2. The concentration of electroluminescent emitters must not be too high to exclude intramolecular effects such as triplet-triplet-annihilation, but the emissive molecules need to act as isolated sites for light generation within the emissive layer as the host material. This material must be inert to the redox and photophysical conditions, and be able to bring both positive and negative charges to the emitters.

Electron Transport Layer (ETL) / Hole Blocking Layer (HBL)

The electron transport layer (ETL) has the identical purpose, as the HTL. However, it is related to the electron transfer *via* LUMO hopping. Suitable materials commonly exhibit electron deficient aromatic compounds such as triazole, imidazoles or pyridines.[75, 78] As this layer is also used to block positive charges from leaving the emissive layer, it can also be called a hole blocking layer (HBL).

Electron Injection Layer (EIL) and Cathode

Again, the electron injection layer (EIL) has the same purpose as the corresponding HIL, but with regard to negative charges transported *via* LUMOs. For this purpose, mixtures of phenanthroline derivatives and quinodimethane derivatives can be used.[83] As the anode is commonly the transparent side of the OLED stack, cheap anode materials such as magnesium, aluminum or alloys of lithium are used.

Fabrication Techniques

Tang and van Slyke used vapor deposition techniques to generate the first OLED.[73] This process offers superior purity of the device as all materials used must be sublimable and can therefore be thoroughly purified by sublimation before the actual device fabrication, which hampers the application of polymers. Another disadvantage is that high-vacuum deposition chambers are costly to maintain especially with panels of increasing size and the fabrication process is batch-based.

Alternatively, solution-based fabrication techniques are explored,[84] as they can offer continuous fabrication processes *via* printing techniques, which are suitable for non-sublimable materials such as heavy emitters or polymers, but a very selective solubility must be present to avoid mixing of layers. To address this issue, cross-linking techniques have been developed.[79, 85]
Ultimately, the operating conditions of OLEDs are harsh as the materials are constantly brought to an oxidized or excited state. For this purpose, reliable encapsulation must be ensured, which is especially challenging if flexible substrates are used.[78]

Out-Coupling of Light

Finally, the generated photon waves propagate in every direction. Only the photons that manage to out-couple through the layers leaving *via* the transparent anode can be seen. The external quantum efficiency (EQE) quantifies the percentage of useable photons.

The multi-layered setup of the device forces the photons to pass several interfaces which exhibit different refractive indices. This can cause refraction and trap the photons within a layer.[86] Specific interface structuring is investigated to enhance the out-coupling by avoiding the refraction.[87]

1.3.1.2 Photophysics of OLEDs

In contrast to excitation *via* photo absorption which selectively yields singlet excited states, electroluminescence is a redox-based process which randomly produces singlet (S_1) and triplet (T_1) excited states. As there are three triplet states and only one excited singlet state, the distribution is 25% *versus* 75% (Scheme 25).

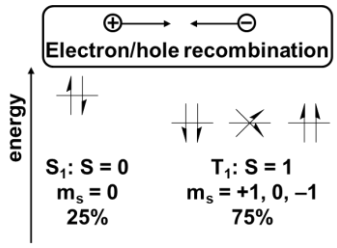

Scheme 25. Quantum statistics state that the multiplicities of the angular momenta m_s form a 25/75 ratio between excited singlet states and triplet states due to the random nature of electron/hole recombination.

As fluorescence is only allowed from the excited singlet state S_1 to the ground state S_0. The maximum quantum efficiency possible is 25% for purely fluorescent compounds. The Jablonski diagram for organic compounds is shown in Scheme 26. Additionally, due to Hund's rule and the spin-orbit coupling, the intersystem crossing (ISC) turns into a competitive mechanism and thus lowers the fluorescence yield.[88] Furthermore, nonradiative relaxation mechanisms (e.g. *via* exciton-phonon coupling[89]), refraction at interfaces and many other losses add up in device, making this system very inefficient.[75]

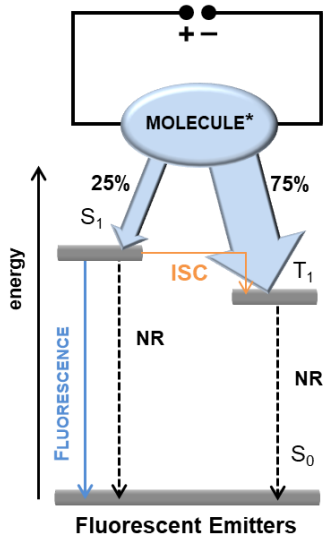

Scheme 26. Jablonski diagram for purely fluorescent emitters. Electric circuit brings a molecule to its excited state indicated with *. The basic pathways of relaxation after electrical excitation include fluorescence or nonradiative relaxation (NR) and intersystem crossing (ISC).

The first generation of OLEDs only using fluorescence to generate light, was soon succeeded by the second generation of OLEDs, where promoted phosphorescence was employed to raise the internal quantum efficiency. As heavy atoms such as iridium or platinum weaken the selection rules by an enhanced spin-orbit coupling, ISC and phosphorescence ($T_1 \rightarrow S_0$) become enabled relaxation pathways as seen in Scheme 27, and the respective emitters are therefore also coined triplet harvesters.[90] In contrast to purely fluorescent emitters, this generation allows to up to 100% of the generated excitons for light generation. Unfortunately, the need of heavy and therefore rare elements makes their use in large scale application expensive.

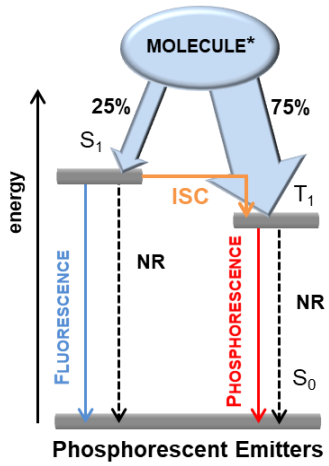

Scheme 27. Jablonski diagram with promoted phosphorescence.

1.3.2 Thermally Activated Delayed Fluorescence (TADF)

The most recent third generation of OLED emitters is able to use all of the available excitons to harvest light as well, but without the need of heavy metal complexes and therefore received much attention in OLED research following the seminal works of Adachi *et al.*[91-94] The so called thermally activated delayed fluorescence (TADF) is now regarded as the most promising mechanism for harvesting excitons[95] in electroluminescent devices. In this concept, the excited S_1 and T_1 states are placed to minimize the energy gap (ΔE_{ST}) (Scheme 28). This permits a rapid equilibration *via* reversed intersystem crossing (RISC) from spin-orbit coupling of isoenergetic levels of S_1 and T_1. Although this mechanism had been known for aromatic ketones, xanthene derivatives and organo-transition metal compounds for a long time,[96-100] it was first considered in OLED research in 2009 by Adachi *et al.* for tin(IV)porphyrin complexes.[91] As OLEDs are operated at ambient temperatures this gap must be small enough to allow efficient RISC at ambient temperature. Adachi *et al.* proposed a ≤ 100 meV criteria for the energetic gap of promising TADF molecules.[93] In principle, it is possible to claim that environmental thermal energy is harvested to generate light.[92]

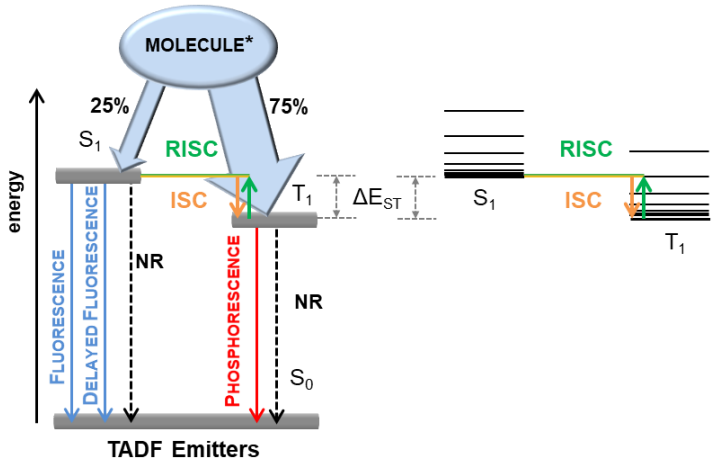

Scheme 28. Jablonski diagram for emitters employing the thermally activated delayed fluorescence (TADF) principle with the ISC/RISC (intersystem crossing and reverse-ISC) emphasized.

Since fluorescence is a considerably faster process than phosphorescence, all excitons can be harvested by (delayed) fluorescent emission. With RISC as the rate determining step, which is only permitted at elevated temperatures, the turn-on of delayed fluorescence (or absence of phosphorescence) can be followed by time-dependant emission decay time measurements (Figure 6).[95, 101]

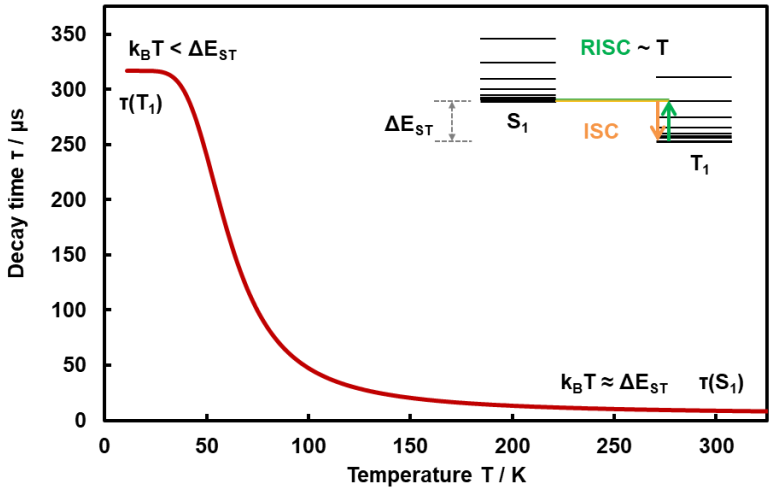

Figure 6. The dependence of the emission decay time τ on the temperature T as proof of TADF. Long decay times in the range of ms indicate an emission *via* phosphorescence, while short decay times (µs) indicate (delayed) fluorescence.[88]

A small ΔE_{ST} is obtained *via* a minute exchange integral between the HOMO and LUMO, as was described by Adachi *et al.*[93, 102] However this can be accompanied by a reduced oscillator strength *f*, which ultimately leads to compromised photoluminescent quantum yield (Φ_{PL}). Therefore, strict design guidelines must be followed to maintain the onset of TADF and the brightness of the emitters (Figure 7).[103] In TADF terminology, the functional moieties containing the HOMO are called donors, while the groups containing the LUMO are named acceptors. These two functional groups are attached to a steric hindrance structure. The vast majority of reported emitters follow a twist principle in order to reduce the overlap of the frontier molecular orbitals (FMOs).[88, 95]

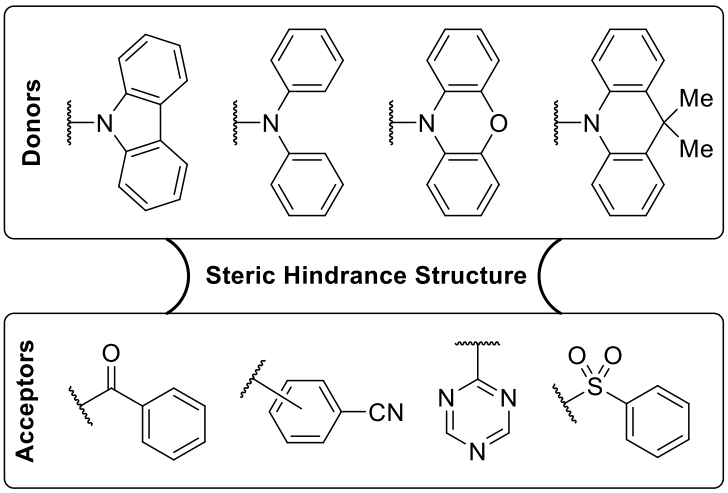

Figure 7. Generic TADF donor and acceptor structures.[88]

A well-known example is the **4CzIPN** emitter (**68**) published by Adachi *et al.*,[93] which shows the reduced overlap *via* concentration of the HOMO mainly on the four carbazole units, while the nitriles

of the isophthalonitrile subunit contain the LUMO. Both orbitals are oriented perpendicularly to each other.

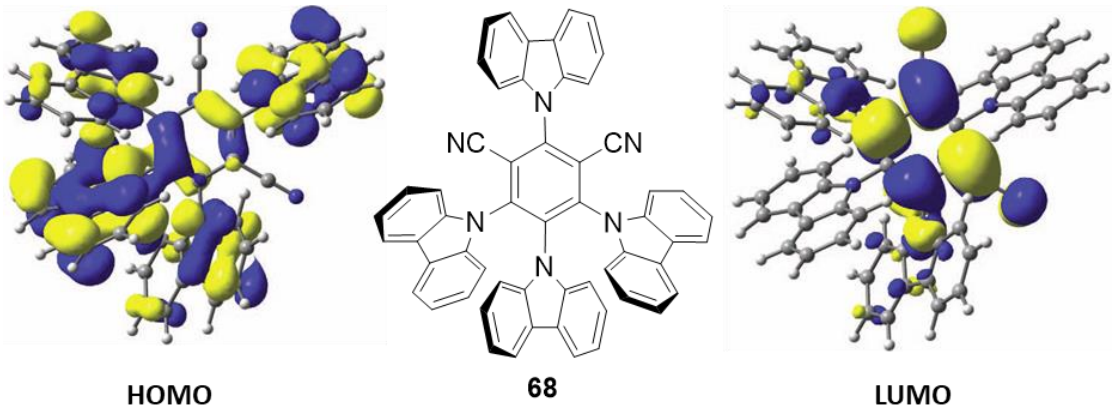

Figure 8. HOMOs are located at the carbazolyl moieties, LUMOs are located at the nitriles. Images taken from Adachi *et al*.[93]

As this research field is very active, recent findings indicate that planar structures are able to exhibit TADF as well, while maintaining a strong oscillator strength.[104-105] This example shows that the details of the TADF mechanism are still under investigation.[106]

Efficient blue emitters are considered as the great goal of OLED research. Molecular TADF design not only relies on large torsions, but also on weak donor units to deepen the HOMO or on weak acceptor units to raise the LUMO. Unfortunately, when both functional moieties are weak, then the frontier molecular orbitals are too dispersed to assure a reduced FMO overlap. A careful balance must be found to obtain performant TADF emitters in the blue region.

1.3.2.1 Through-Space Design

A less explored, but striking design concept for TADF that has been investigated mainly by Swager, Baldo *et al.* is the electronic communication of donor and acceptor groups mediated by through-space conjugation. This excludes spiro-linked emitters which allow an electronic communication *via* one sp^3-center. So far, a triptycene skeleton confining the donor and acceptor units in a 120° orientation,[107] and a xanthene-linked cofacial orientation of the donor and acceptor with a distance of 3.3–3.5 Å were reported (Figure 9).[108] In case of the triptycene emitters **69** and **70** a τ_D of 6.5 µs and 2.4 µs was observed, respectively, which is in accordance with the small ΔE_{ST} values calculated. As the oscillator strength (*f*) is calculated without considering through-space interaction, it can be taken as an indicator of how exclusive this through-space interaction is with respect to luminance. OLED devices were fabricated, showing EQE_{max} values of 4.0% and 9.4% in the green (542 nm) and yellow (573 nm) range. Six donor-expanded derivatives of **69** were reported by Geng, Su *et al.* in silico, with the smallest ΔE_{ST} of 26 meV for a *tert*-butylcarbazole derivative.

Following the xanthene-bridged donor/acceptor design, emitters **71**–**73** were reported, with even smaller oscillator strengths of 0.0001-0.008, yet accompanied by minute ΔE_{ST} values of 0.1–8 meV. As the carbazole emitter **72** showed reduced stability, only OLEDs with the phenoxazine donor **71** and the *tert*-butylcarbazole donor **73** were fabricated with again moderate EQE_{max} values of 10% and 4% in the yellow (584 nm) and sky-blue (488 nm) spectrum. Although TADF was observed with delayed lifetimes, τ_D of 3.3 µs and 4.1 µs accompanied by moderate Φ_{PL}, the through-space electronic communication mainly occurred *via* C–H···π interactions, creating efficient aggregation induced emission.

As the design of a through-space mediated TADF emitter based on a [2.2]paracyclophane core was a main target of this thesis (*vide infra*), the results of a competing group are mentioned in Figure 9. The results of that group were published after the completion and publication of excerpts of this thesis.[109] Recently, Zhao *et al.*[110] reported on [2.2]paracyclophane-based through-space mediated TADF emitters with a pseudo-*geminal* and a pseudo-*meta* orientation of the dimethylamino donor and dimesitylboron acceptor yielding **74** and **75**. This design gave increased ΔE_{ST} values compared to the xanthene and triptycene design, but increased through bond oscillator strengths in the range of **70**. As the reported τ_D values of 0.38 µs and 0.22 µs for emitters **74** and **75**, respectively, are questionably low in order to claim the turn-on of TADF, no devices were fabricated. But chiral separation of the racemic emitter **74** showed distinct CPL emission for each enantiomer with a maximum g_{lum} value of 4.24×10^{-3}.

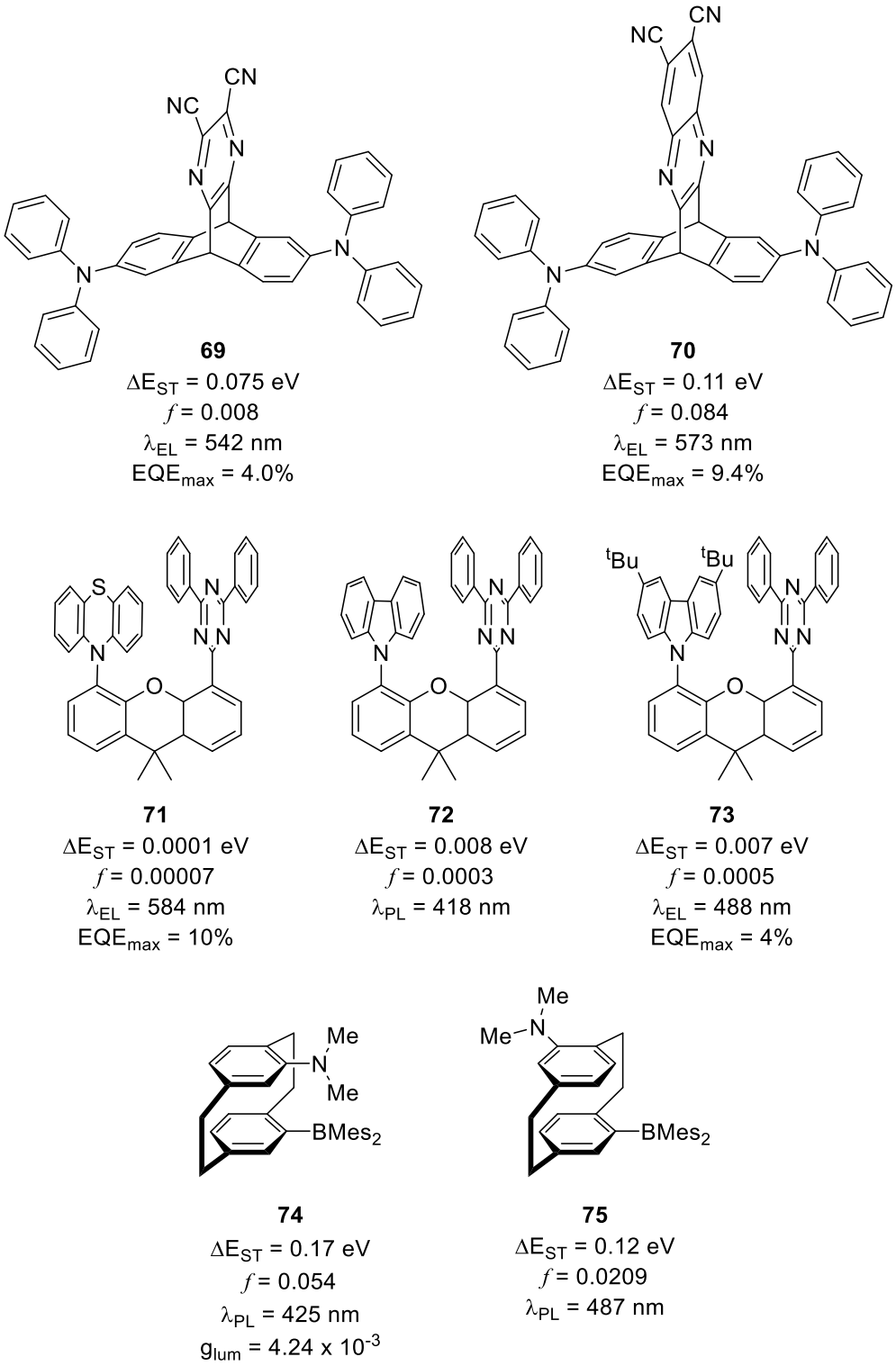

Figure 9. Overview of reported through-space TADF emitters.[107-108, 110]

1.3.2.2 Triazine Twist Design

The turn-on of TADF *via* twisting can be exemplified with the TADF research conducted on the simple *N*-carbazolyl-4-triphenyltriazine D–A structure **76** (Figure 10). This structural class commonly does not display low oscillator strengths. As the parent compound shows deep-blue photoluminescent emission of 381 nm, which is a key goal of OLED research, it does not exhibit TADF due to a HOMO–LUMO splitting of 0.30 eV, which does not meet the criteria for an efficient RISC process.[111] Early attempts to optimize this structure were conduction by substitution of the donor unit to phenoxazine yielding **77**,[112] or dimethylacridine yielding **78**.[113] A significant decrease of ΔE_{ST} to 0.07 and 0.05 meV was reported, accompanied by a significant increase of the torsion angle to 74.9° and 88° for the respective emitters. This can be explained by the increased proximity of the *ortho*-hydrogen atoms caused by the increased size of the six-membered 1,4-oxazine and 1,4-(4,4'-dimethyl)dihydropyridine subunits compared to the five-membered pyrrole subunit in the carbazole donor of **76**. The change of structure, conformation and ultimately the energetic profile of emitters **77** and **78** resulted in TADF turn-on proven by device performances (EQE_{max}) of 12.5% and 26.6%, although a large red-shift to blue-green (500 nm) and green (529 nm) was observed. To stay in the blue region, clearly the weak carbazole donor unit was to be kept, but an increase of twist was needed. To meet these criteria, emitters with methyl groups at the *ortho*-positions to the N–C bond were introduced by Adachi *et al.* to yield emitters **79**–**81**.[114] All emitters showed a distinct torsion angle of 71.3°–86.7°, ΔE_{ST} of 0.08–0.17 eV and excellent device performances (EQE_{max}) of 18–22%. Only emitters **80** and **81** managed to give deep-blue electroluminescence of 450 nm and 452 nm, respectively, while emitter **80** showed a significant red-shift to 500 nm. This can be explained by the dramatically reduced ionization potential of the 1,3,6,8-tetramethylcarbazole, making the triplet state a stable ^{3}CT (charge transfer) state rather than a ^{3}LE (locally excited) state. Swager *et al.* introduced a triptycenylcarbazole unit to determine if the HOMO–LUMO splitting can be reduced effectively without lowering the S_1 state needed for deep-blue emission *via* homoconjugation.[115] The resulting emitters **82** and **83** showed decreased torsion angles of 51.6° and 69.5° and worse device performances of (EQE_{max}) 10.4% and 11%, respectively when compared to emitters **79**–**81**. When emitter **82** is compared to the parent compound **76**, a TADF turn-on could be achieved by expansion of the HOMO without introducing additional torsion to the system with a delayed emission lifetime (τ_d) of 38 µs for **82** and no detected delayed emission component for **76**. Finally, emitter **83** proves that additional torsion is the most straight forward method to reduce ΔE_{ST}.

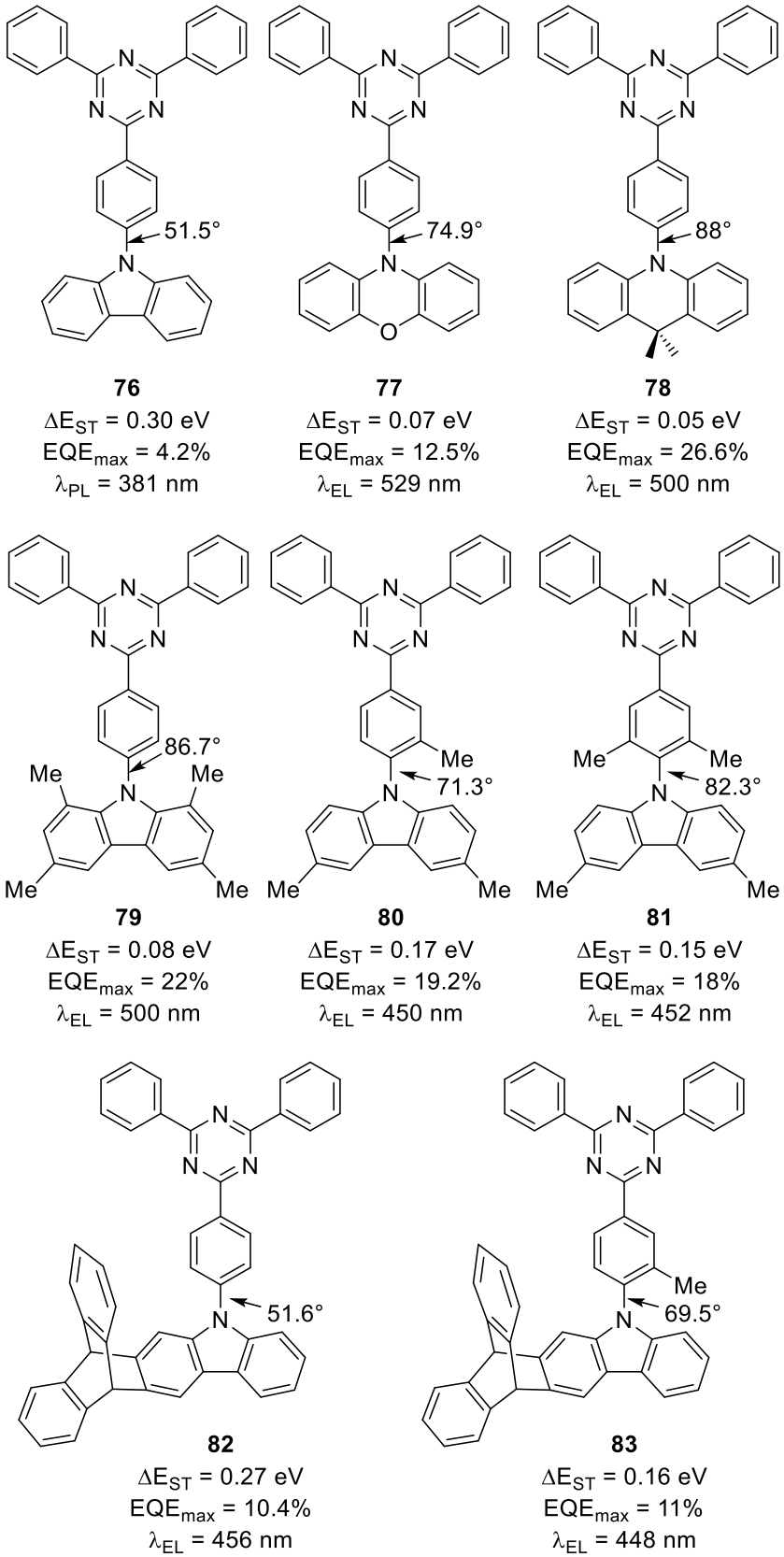

Figure 10. Overview of published examples of TADF turn-on of the parent triazine emitter **76**. All values are given from the reported device architectures and all torsion angles are reported from DFT calculations.[111-115]

2 Objective

Since the first discovery of [2.2]paracyclophane (**1**) by Brown and Farthing exactly 70 years ago[1] as a byproduct of the pyrolysis of *para*-xylene,[26] this molecule has sparked tremendous interest in the scientific community. The two co-planar phenyl rings in close proximity of 3.09 Å,[2-3] fixed by two short ethyl bridge units in *para*-position result in a "*bent and battered*"[2] molecular skeleton which is unknown in conventional non-cyclophane aromatic chemistry. The key features of this molecule are I) the unique electronic situation enabling transannular electronic communication of the two π -systems,[4-5] II) the presence of planar chirality upon substitution and III) the considerable spherical bulk induced by the adjacent ethyl bridge and second coplanar phenyl ring. Despite these unique features, the bent and therefore unfavored conformation influences the chemistry of this molecule dramatically, making the synthetic access to desired molecules a challenging endeavor.
Up until now the [2.2]paracyclophane scaffold has predominantly been investigated in catalysis as a chiral ligand,[7-9] exploiting the chirality and steric hindrance of this molecule. An example of this is the commercialization of the chiral [2.2]paracyclophane-based phanephos ligand.[116] In contrast, investigations regarding material sciences are far less explored.[6]

Therefore, the aim of this thesis was to establish a synthetic access to [2.2]paracyclophane-based derivatives for different applications in material sciences and supramolecular chemistry (Figure 11).

In the first project, thermally activated delayed fluorescence (TADF) emitters are synthesized with the [2.2]paracyclophane serving as a bridge between an electron rich and an electron poor aromatic substituent to mediate through-space electronic communication. For this, a synthetic access to pseudo-*geminal* and pseudo-*para* oriented functional groups has to be developed. Since no general cross-coupling protocol is known, and steric hindrance for the pseudo-*geminal* emitter group is expected, these syntheses must be carefully optimized.
Additionally, a second class of TADF emitters is designed and synthesized using the [2.2]paracyclophane as an extension of the electron rich (1,4)carbazolophane donor group in combination with a triazine acceptor unit to turn-on the TADF mechanism. Furthermore, the chirality of the resulting emitter which is introduced by the substituted [2.2]paracyclophane scaffold should be evaluated through a stereoselective access to this emitter.

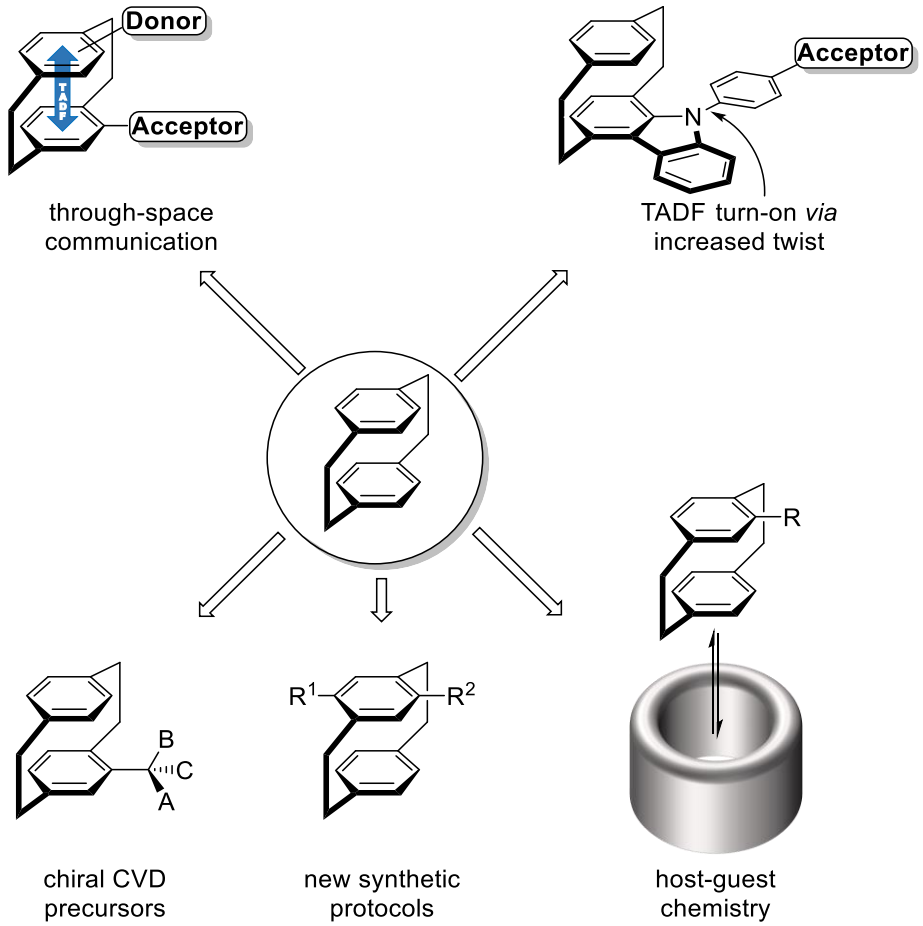

Figure 11. Objectives of this thesis.

In a second project, new [2.2]paracyclophane-based chemical vapor deposition (CVD) monomers are synthesized in order to tackle the recently posed question, whether it is possible to transfer chirality from a CVD monomer to a parylene polymer, for this the access to enantiopure derivatives is be explored.

Finally, the assumption that certain substituted [2.2]paracyclophanes can be promising guest molecules in supramolecular chemistry with cucurbit[8]uril has to be verified by evaluation of a suitable synthetic access to 4-(4’-pyridyl) derivatives.